PAPER • OPEN ACCESS

Effects of time on the evolution of a wave packet in the tunneling dynamics

To cite this article: Lijuan Jia *et al* 2021 *New J. Phys.* **23** 113047

New Journal of Physics
The open access journal at the forefront of physics

Deutsche Physikalische Gesellschaft DPG
IOP Institute of Physics

Published in partnership with: Deutsche Physikalische Gesellschaft and the Institute of Physics

OPEN ACCESS

RECEIVED
23 July 2021

REVISED
23 October 2021

ACCEPTED FOR PUBLICATION
15 November 2021

PUBLISHED
30 November 2021

PAPER

Effects of time on the evolution of a wave packet in the tunneling dynamics

Lijuan Jia[1], **Long Xu**[2], **Peng Zhang**[3,*] **and Libin Fu**[1,*]

[1] Graduate School of China Academy of Engineering Physics, No. 10 Xibeiwang East Road, Haidian District, Beijing, 100193, People's Republic of China
[2] AMOS and Department of Chemical and Biological Physics, The Weizmann Institute of Science, Rehovot 7610001, Israel
[3] Department of Physics, Renmin University of China, Beijing 100872, People's Republic of China
[*] Authors to whom any correspondence should be addressed.

E-mail: pengzhang@ruc.edu.cn and lbfu@gscaep.ac.cn

Keywords: tunneling dynamics, temporal evolution of wave packet, Loschmidt echo function, characteristic time

Abstract

We investigate the time-dependent electron wave packet in a one-dimensional geometry with the potential bent by a homogeneous external field. Based on the behaviors of the wave packet over time, we observe a crossover time. After this crossover time, the temporal evolution of the wave packet comes into a new regime, where the wave packet evolves in a self-similar structure. To establish the time scale of this crossover quantitatively, we utilize the Loschmidt echo function, through which the time at which the crossover occurs can be extracted. We also find the time of the maximum ionization velocity can be comparable with the semi-classical tunneling delay time.

1. Introduction

Tunneling is a striking phenomenon in quantum physics, which was addressed in many areas of science, such as condensed matter physics [1–5], optics [6–8], and attosecond physics [9–11]. The dynamics of tunneling is at the heart of understanding the general quantum tunneling process and has been a hotly debated topic over decades, while the issue of tunneling time attracting the most attention has remained contentious [12–14] since it was first put forward by MacColl [15]. More recently, this issue was triggered again in the field of the interaction between atoms and strong laser pulses, where the dynamics of ionized electrons can be tracked experimentally on the attosecond scale by a powerful angular streaking technique [16, 17]. It determines a tunneling delay time by a streaking angular offset, which is the angle of rotation in the electron momenta distribution, relative to what would be expected if the most probable electron trajectory appears at the tunnel exit at the peak of the laser field.

Tunneling dynamics is served as a fundamental process in many different physical fields. Viewed as a dynamical event, it is very natural to associate a characteristic time with tunneling in quantum mechanics. And the determined tunneling time would be related to a specific setup for the wave function and a specific defining scheme. For instance, McDonald, Orlando *et al* [18, 19] have proposed a tunneling time spent by the dynamic resonance state isolated from the total wave function reaching a constant ionization rate. In solid physics, Niu [20] showed a tunneling time describing the regime of the temporal evolution of the survival probability of the lowest band changing from strong oscillation to exponential decay. Besides, other tunneling times used to characterize the temporal evolution of wave packets have also been defined in different physical contexts [21–23].

Still, all of these defined characteristic times are determined by the energy width of the ground state, induced by an external field or an accelerating potential. However, so far, a detailed description of the time-dependent evolution of the total electron wave packet in the tunneling dynamics is lacking. And a tunneling time characterizing the evolution of the total electron wave packet in the presence of a perturbation is undetermined.

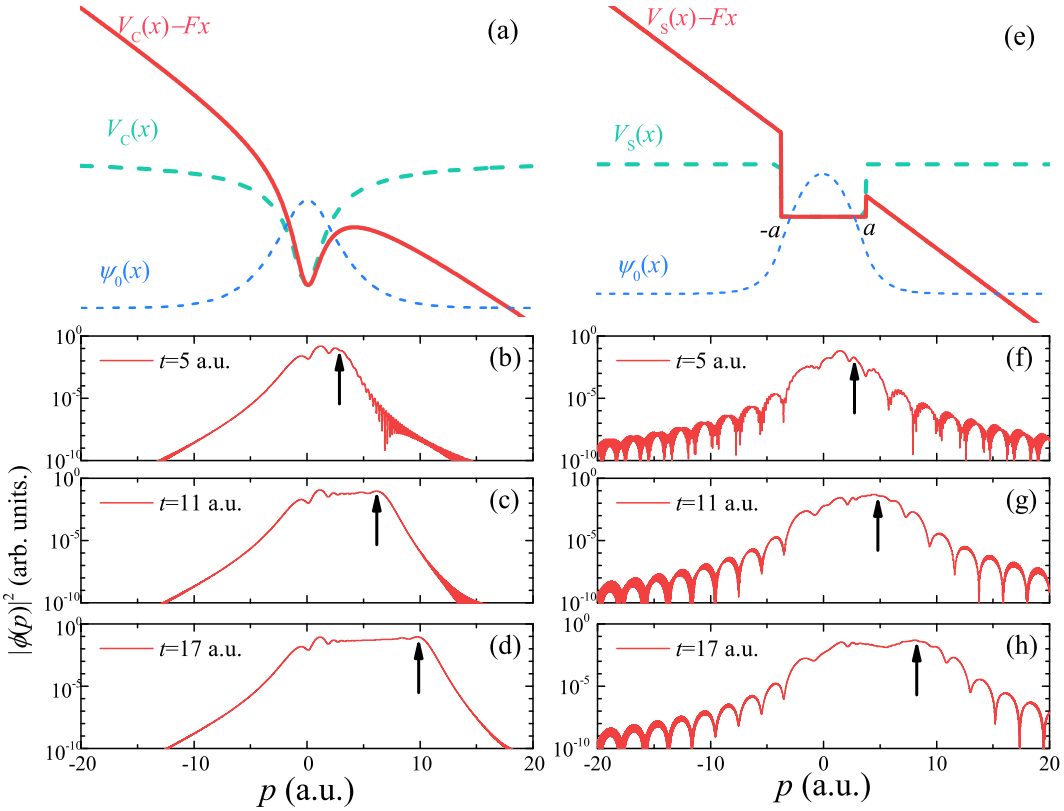

Figure 1. Left panel: (a) the one-dimensional Coulomb potential $V_C(x)$, which defines the effective potential $V_C(x) - Fx$ by applying an external field F. $\psi_0(x)$ is the ground state. The momentum distributions with $F = 0.6$ a.u. at (b) $t = 5.0$ a.u., (c) $t = 11.0$ a.u. and (d) $t = 17.0$ a.u. The arrows show the positions of the wavefront. Right panel: the same statement with left panel except that the Coulomb potential is replaced by the square well potential.

In this paper, we aim to study the temporal evolution of an electron wave packet in a full quantum mechanical approach. By solving the time-dependent Schrödinger equation (TDSE) and analyzing the ionized wave function, we find that the evolution of the wave packet steps into a new regime after a crossover time, at which the wave packet starts to evolve in a self-similar structure. We define this crossover time obtained from the dynamical evolution of electron wave packet as the tunneling time. To distinguish the different evolution stages of the wave packet, we quantify this crossover time by applying the Loschmidt echo function [24, 25]. We also study the time of the maximum ionization velocity (MIV) and find it is of the same magnitude as the semi-classical tunneling delay time.

The paper is organized as follows. In section 2, we introduce our model for a homogeneous external field. In the presence of an external field, the temporal evolution of wave packet is discussed in section 3. Afterwards, we propose a method to characterize the tunneling dynamics of a wave packet in section 4. Finally, we draw our conclusions in section 5. Atomic units are used throughout the paper unless stated otherwise.

2. Theoretical methods

Most of the works [18, 26, 27] that have so far dealt with the tunneling problem have investigated reduced-dimensionality (1D) systems. The reason for this treatment is that the electric dipole approximation is applied in tunneling theories, and the effect due to the magnetic field component is ignored [28]. Thus, the linear polarization of the electric field renders the motion of the electron quasi-one dimensional, allowing us to investigate general features of tunneling in one-dimensional (1D) scenario. In what follows, we consider the electron trapped in a 1D potential exposed to a homogeneous electric field $F(F > 0)$. Here, two different potentials, atomic Coulomb potential and square well potential, are employed [see figures 1(a) and (e)]. The square well potential is a short-range potential, while the Coulomb potential is a long-range potential and its tail effect always entangles with the tunneling dynamics in strong-field ionization of atoms. Hence, by comparing the results of these two potentials, the tail effect can also be studied.

For the atomic Coulomb potential, the Hamiltonian of the system takes the form

$$H = -\frac{1}{2}\frac{\partial^2}{\partial x^2} + V_{\rm C}(x) - Fx, \tag{1}$$

where $V_{\rm C}(x) = -1/\sqrt{x^2+b^2}$ represents the soft-core electron–nucleus interaction [29, 30] with b as the soft parameter. The unperturbed ground state $\psi_0(x)$ is set as the initial state, and the TDSE is numerically solved by the split-operator method [31].

We also use a square well potential $V_{\rm S}(x)$ with the depth $-V_0$ and the width $2a$, as shown in figure 1(e), where the triangular barrier is formed by combining the square well potential with the external field. The eigenvalue equation of this system is given by

$$\left(-\frac{1}{2}\frac{\partial^2}{\partial x^2} + V_{\rm S}(x) - Fx\right)\psi_{\rm E}(x) = E\psi_{\rm E}(x), \tag{2}$$

where E is the eigenvalue, ranging from $-\infty$ to ∞, and $\psi_{\rm E}$ is the corresponding eigenfunction. By introducing a parameter $\xi(x) = (x + E/F)(2F)^{1/3}$, the above equation [equation (2)] can be solved analytically and the solutions are given by

$$\psi_{\rm E}(x) = \begin{cases} Z_{\rm E}^{(-)}A_i[-\xi(x)], & x \leqslant -a, \\ \alpha\,\sin(\eta x) + \beta\,\cos(\eta x), & -a < x < a, \\ Z_{\rm E}^{(+)}A_i[-\xi(x)] + N_{\rm E}^{(+)}B_i[-\xi(x)], & x \geqslant a, \end{cases} \tag{3}$$

where $\eta = \sqrt{2(E+V_0)}$ for $E + V_0 \geqslant 0$, and $\eta = i\sqrt{-2(E+V_0)}$ for $E + V_0 < 0$. Here $A_i(x)$ and $B_i(x)$ are two linear-independent Airy functions [32]. The five unknown parameters in the above equation are determined by four continuity conditions that $\psi_{\rm E}(x)$ and its derivative are continuous at $x = \pm a$, and by a normalization condition $Z_{\rm E}^{(+)2} + N_{\rm E}^{(+)2} = (4/F)^{1/3}$, rooted in the outgoing bound condition [32]. Then, by expanding the initial state (the unperturbed ground state) $\psi_0(x)$ in the basis of these eigenfunctions, $\psi_{\rm E}(x)$, the time-dependent wave function $\psi(x,t)$ can be written as

$$\psi(x,t) = \int_{-\infty}^{\infty} {\rm d}E g(E) {\rm e}^{-{\rm i}Et}\psi_{\rm E}(x), \tag{4}$$

where $g(E) = \int {\rm d}x \psi_{\rm E}^*(x)\psi_0(x)$ denotes the spectral probability amplitude.

Over time, the electron can tunnel through the potential barrier formed by combining the atomic Coulomb potential or the square well potential with the electric field's potential, and subsequently be ionized. The ionized wave function for both systems is given by

$$\psi_{\rm ion}(x,t) = \psi(x,t) - \sum_i \langle\psi_i(x)|\psi(x,t)\rangle\psi_i(x), \tag{5}$$

where $\psi_i(x)$ represents the ith ($i = 0, 1, 2, \ldots$) unperturbed bound state.

To make results of the two systems better comparable, we set the same ionization energy $I_{\rm p} = 1.696$ a.u., where $b = 0.097$ a.u., $V_0 = 2.0$ a.u., and $a = 1.5$ a.u. Note that there are two bound states, the even- and odd-parity states, in the system of square well potential. In this work, the external field F ranges from 0.5 a.u. to 1.0 a.u., corresponding to the intensity I_0 changing from 8.75 to 35.01×10^{15} W cm^{-2}.

3. Temporal evolution of an electron wave packet

In the tunneling ionization (TI), an electron is ionized by an external field and escapes from the potential barrier formed by combining the Coulomb potential or the square well potential with the external field; see figures 1(a) and (e). The photoelectron momentum distributions at three different times for the two systems are also plotted in figure 1. With time, the wave packet spreads rightwards in the momentum space and the width of momentum distribution increases, which implies the increase of the average momentum of the system. This increase in the momentum coincides with the motion of classical electrons in the external electric field. In a semi-classical counterpart, the ionized electrons will be continuously accelerated by the homogeneous electric field. Apart from a highest peak around $p = 0$, which keeps its position constant, there exists a visible moving peak with the spread of ionized wave packet for both cases. We call this rightwards propagating peak in the region of $p > 0$ as wavefront [see the positions of arrows in figure 1]. At the same time, in coordinate space, wavefront denotes the rightwards propagating peak of probability density $|\psi_{\rm ion}(x)|^2$ with time in the region of $x > 0$.

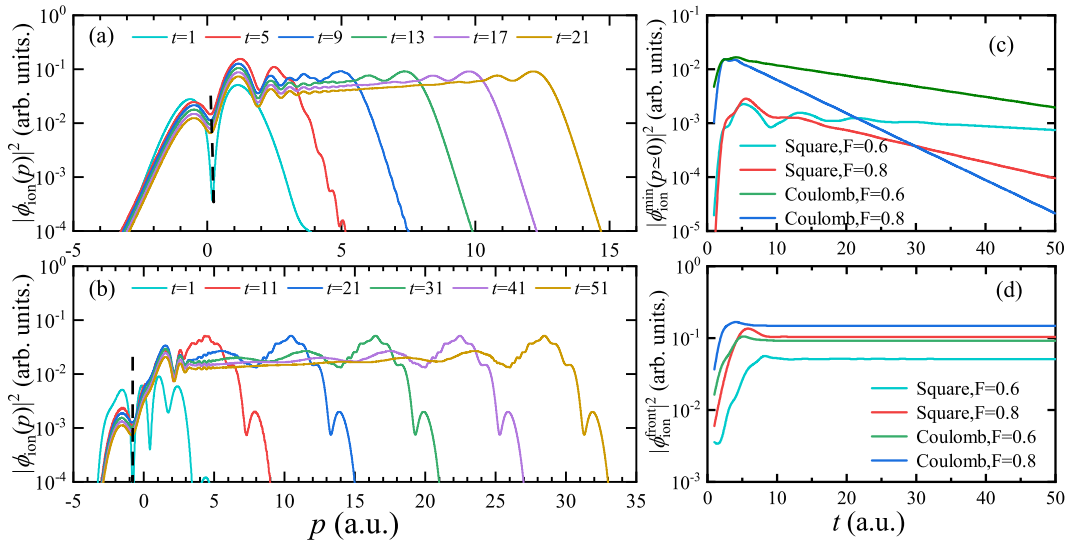

Figure 2. The momentum distributions at different times for the systems of (a) Coulomb potential and (b) square well potential with $F = 0.6$ a.u. (c) The minima of $|\phi_{\rm ion}(p \simeq 0)|^2$ marked by the dashed black line [see (a) and (b)] with respect to time. (d) The probability of the wavefront of momentum distribution as a function of time.

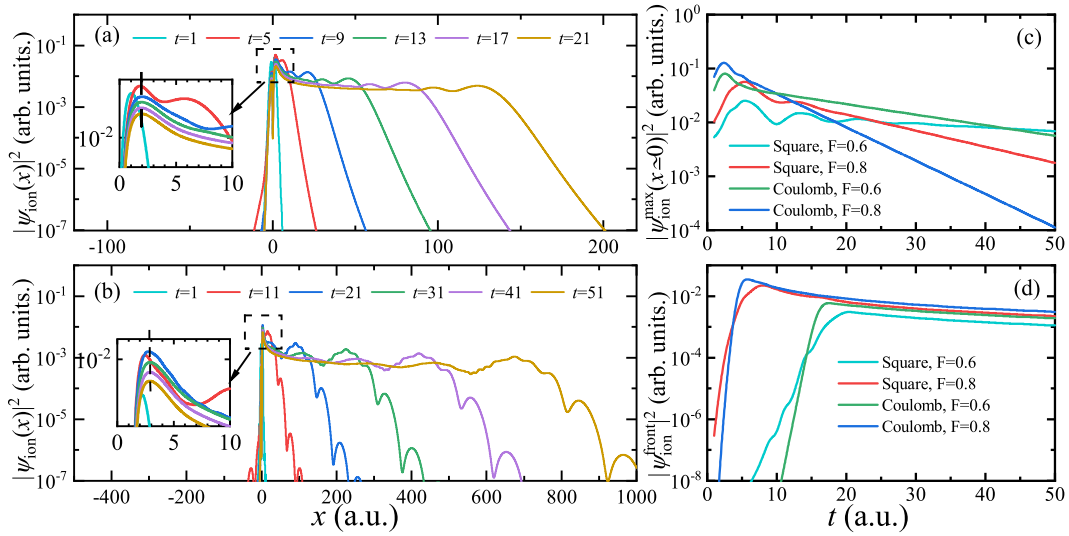

Figure 3. The ionized wave function for the cases shown in figure 2 except that (c) the maxima of $|\psi_{\rm ion}(x \simeq 0)|^2$ as a function of the evolution time. The insets show a magnified portion.

To study the dynamics of electrons in the tunneling regime in detail, we plot the momentum distributions at different times in figures 2(a) and (b), taking $F = 0.6$ a.u. as an example. Two prominent features of the time-dependent wavefunction are observed, which shows that the phenomena in both cases are similar. One appealing feature is the time-dependent behavior of probability density $|\phi_{\rm ion}(p)|^2$ in the vicinity of $p = 0 (p \in (-1, 1))$. It can be clearly seen in figure 2(c), where we plot the local minima of $|\phi_{\rm ion}(p)|^2$ [see the black dashed lines in figures 2(a) and (b)] as a function of time. It shows that initially $|\phi^{\rm min}_{\rm ion}(p \simeq 0)|^2$ oscillates and then decays exponentially with time. This phenomenon is similar to that of the variation of survival probability over time for atoms in an accelerating optical lattice [20]. As to the coordinate wave functions, $|\psi_{\rm ion}(x)|^2$, shown in figures 3(a) and (b), we also consider the temporal behavior of probability density $|\psi_{\rm ion}(x)|^2$ in the region of around $x = 0 (x \in (0, 10))$ [see the inserts in figures 3(a) and (b)] and plot the local maxima of $|\psi_{\rm ion}(x)|^2$ as a function of time in figure 3(c). We find that it coincides with the behavior of the minima in the momentum distribution [see figure 2(c)]. It should be noted that it is reasonable to figure out the maximum probability density $|\psi_{\rm ion}(x)|^2$ simultaneously. The partial electron wave packets in the coordinate space and momentum space are uncorrelated, while the electron wave packets in the whole coordinate space and momentum space are interdependent.

The other outstanding feature is the variation behavior of wavefront. Figure 2(d) shows the probability density of the wavefront as a function of time. One can see that initially, the value $|\phi_{\rm ion}^{\rm front}|^2$ rapidly rises at the beginning and later keeps constant. It seems that for longer times, the wavefront translates rightwards uniformly [also see figures 2(a) and (b)]. For square well potential, the ionized part of wavefunction is merely subjected to the uniform electric field. It inspires us to calculate a quantum model that a free electron interacts with a uniform electric field to explain and quantify the motion of the ionized wavefront. The Hamiltonian of this model can be written as $H_{\rm free} = p^2/2 - Fx$. For an arbitrary initial state $|\psi_{\rm a}\rangle$, its time-dependent wave function in the momentum space is given by $\phi(p,t) = \langle p|{\rm e}^{-{\rm i}H_{\rm free}t}|\psi_{\rm a}\rangle = {\rm e}^{-{\rm i}tp^2/2}$ ${\rm e}^{{\rm i}t^2Fp/2}{\rm e}^{{\rm i}t^3F^2/3}\langle p|{\rm e}^{{\rm i}Ftx}|\psi_{\rm a}\rangle$. As a result, the momentum distribution satisfies

$$|\phi(p,t)|^2 = |\langle p - Ft|\psi_{\rm a}\rangle|^2 = |\phi(p-Ft,t)|^2. \tag{6}$$

which manifests that the momentum wave function of a free electron will translate rightwards with an acceleration F, while keeping its shape; see figure 2(b). Therefore, for the short-range square well potential, the probability density of the wavefront will undoubtedly remain unchanged [see figure 2(d)] as the electron tunneling out the potential barrier. However, in the case of Coulomb potential, for long times, the wavefront behaves the same as that of square well potential, as shown in figures 2(a) and (d). Also, if one compares the snapshots of wavefunction for $t = 21$ a.u. in figures 2(a) and (b), the wavefront momenta for both Coulomb potential and square well potential are approximately the same. These indicate that the tail of the long-range Coulomb attractive potential can be taken as a perturbation when the electron is away from the parent ion.

Also, figure 3(d) depicts the dependence of the probability density of wavefront on time. Unlike the behavior of wavefront in the momentum distributions [see figure 2(d)], the probability density of wavefront for the coordinate wave functions initially performs a rapid rise, then decreases smoothly for longer times. The decrease is due to the spread of wave packets of different momentum components in the coordinate space. In coordinate space, the wavefront undergoes a uniformly accelerated linear motion with an acceleration equal to F. Together with the motion of wavefront in momentum space, the behaviors of the ionized wavefront coincide with the motion of a free electron subjected to a constant electric field in classical picture. It shows again that the motion of a microscopic quantum ionized wave packet can be intuitively understood from a viewpoint of a macroscopic classical particle.

From figures 2 and 3, a regular evolution regime of wavefunction is established when the temporal behavior of probability density around zero is no longer oscillating but decaying exponentially and the probability density of wavefront starts to remain unchanged in momentum space or fall smoothly in coordinate space. This yields that the shape of the wave functions at different times looks similar, namely, the wave functions adjust themselves to the field. We mark this regular evolution regime as the steady state of the system and define the corresponding time as the crossover time of the system. Note that the quantum dot potential is also a short-range potential. It results in that the evolution behavior of time-dependent wavefunction for quantum dot potential will resembles with that of square well potential. As expected, a similar structure of wave packet for long times in the case of a 1D quantum dot potential has been observed [18, 19].

4. Characterization of the crossover time of wave packet dynamics

As discussed above, the tunneling dynamics of the wave packet comes into a steady state and evolves in a self-similar structure after the crossover time. Note that this behavior is in qualitative agreement at different reference points around $x = 0 (p = 0)$ and the neighboring points of wavefront. Hence, though this time can be directly read from figures 2 and 3, it is point-dependent with a relative error less than 0.58 pencent. To quantitatively describe the similarity of the ionized electron wave packet at different times and quantify the crossover time uniquely, we employ the Loschmidt echo function [24, 25]

$$L(t;{\rm d}t) = |\int_{-\infty}^{\infty} {\rm d}x\psi_{\rm ion}^*(x,t)\psi_{\rm ion}(x,t+{\rm d}t)|^2, \tag{7}$$

which is extensively used to describe the similarity of two different states.

Corresponding to the normalized and unnormalized ionized wave functions $\psi_{\rm ion}$, we can define two types of Loschmidt echo function, $L^{\rm N}$ and $L^{\rm UN}$, respectively. $L^{\rm N}$ only contains the information of the shape fidelity of the ionized wave function, while in the unnormalized case, $L^{\rm UN}$ also reflects the mode change of the wave function. Figure 4 plots the Loschmidt echo functions, $L^{\rm N}$ and $L^{\rm UN}$ as a function of time for $F = 0.6$ a.u. Both $L^{\rm N}$ and $L^{\rm UN}$ eventually tend to 1 for the small dt in equation (7). With d$t = 0$, equation (7) reduces to ionization probability at the instant t. In the well-known Landau–Zener tunneling,

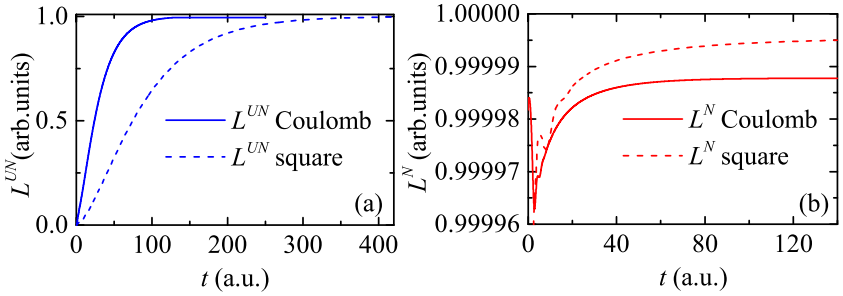

Figure 4. (a) L^{UN} and (b) L^{N} as a function of time for the systems of Coulomb potential and square well potential with $F = 0.6$ a.u. and $\mathrm{d}t = 0.01$ a.u.

the survival probability of the lowest band exhibits an exponential decay for long times [20]. Also, the time-dependent probability density around zero decays exponentially for long times [see figures 2(c) and 3(c)]. Thereby, to extract the crossover time from figure 4, the Loschmidt echo function is fitted as $L(t;\mathrm{d}t) = A\mathrm{e}^{-t/T_{\mathrm{c}}} + B$ without considering some data for relatively short times. Then, the crossover time, T_{c} of the system is determined by a unified norm that T_{c} is the time satisfying $L(t;\mathrm{d}t) \propto \mathrm{e}^{-1}$. Careful calculations are performed to show that T_{c} is convergent with respect to the parameter $\mathrm{d}t$. And for the normalized and unnormalized cases, one can see the crossover times differ significantly.

Specifically, we can verify analytically that the L^{UN} reflects the ionization process in essence. Substituting equation (5) into (7), as $\mathrm{d}t$ is small ($\mathrm{d}t$ is less than 0.01 a.u. in our model), we can expand L^{UN} to first order in perturbation,

$$L^{\mathrm{UN}} = \left|1 - a(t) + ib(t)\mathrm{d}t - i\mathrm{d}t\int_{-\infty}^{\infty}\mathrm{d}E|g(E)|^2E\right|^2, \tag{8}$$

where

$$a(t) = \int_{-\infty}^{\infty}\mathrm{d}E'\int_{-\infty}^{\infty}\mathrm{d}E|g(E)|^2|g(E')|^2\mathrm{e}^{-\mathrm{i}(E-E')t},$$
$$b(t) = \int_{-\infty}^{\infty}\mathrm{d}E'\int_{-\infty}^{\infty}\mathrm{d}E|g(E)|^2|g(E')|^2\mathrm{e}^{-\mathrm{i}(E-E')t}E.$$

Here $1 - a(t)$ and $-2\,\mathrm{Im}[b(t)]\mathrm{d}t$ represent the ionization rate and its change, respectively, and $2\,\mathrm{Re}[b(t)]\mathrm{d}t - \int \mathrm{d}E|g(E)|^2E\mathrm{d}t$ is the total phase change of the ionized wave function. Interestingly, the time T_{c} determined by $a(t)$, $\mathrm{Re}[b(t)]$ or $\mathrm{Im}[b(t)]$ is nearly equal to T_{c} calculated by L^{UN} [equation (8)] according to the exponential fitting formula $A\mathrm{e}^{-t/T_{\mathrm{c}}} + B$, considered above.

Also, we calculate the time-dependent ionization velocity $(|\psi_{\mathrm{ion}}(t+\mathrm{d}t)|^2 - |\psi_{\mathrm{ion}}(t)|^2)/\mathrm{d}t$ for the two systems. And the ionization velocity is equal to $-2\,\mathrm{Im}[b(t)]$ [see equation (8)] for square well potential. The time of the MIV is denoted as T_{MIV}, which is a full-quantum time. By contrast, the time of maximum probability current (MPC) at the tunneling exit is also calculated. This position-dependent time T_{MPC} is obtained by setting $t_0 = 0.0$ (the time when the field strength reaches the maximum) and it right corresponds to the tunneling time delay τ_{A} defined in reference [26].

Figure 5 presents the various typical times as a function of field strength. As can be seen, the crossover time is, especially for weaker F's, several orders of magnitude higher than the other times (T_{MIV} and T_{MPC}) and decreases much faster with increasing the field strength. This points to the important difference between the definitions of the crossover time and the other times. The crossover time, extracted from the time-dependent behavior of probability density reflects the time needed by a majority parts of wavefunction to escape through the barrier. As shown in the inset of figure 5, the ionization probability $[P_{\mathrm{ion}} = 1 - |\langle\psi_0|\psi(t)\rangle|^2]$ at the crossover time is more than 60% for both systems of Coulomb potential (blue line) and square well potential (blue-dashed line). Such high ionization probability results in that the crossover time will be extremely sensitive on the barrier shape and barrier wall, created by the superposition of the bare potential and the laser field. A larger electrostatic field bends the barrier lower and narrower, providing a chance for the electron escaping from the barrier faster. Thus, the crossover time is more easily achieved for a stronger field strength. Whereas the other times (T_{MIV} and T_{MPC}) reflect the time needed by a small fraction of wavefunction to pass the barrier. They will be much smaller and are less sensitive on the barrier width than the crossover time.

Moreover, the crossover times for L^{N} and L^{UN} in the system of the square well potential are always greater than that of the Coulomb potential in the field range, although the general features are the same.

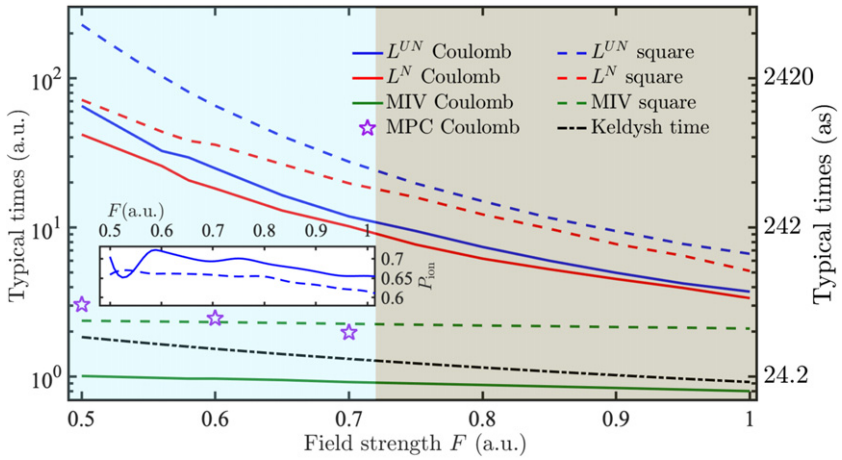

Figure 5. Kinds of typical times as a function of field strength F for the systems of Coulomb potential and square well potential. The times of maximum probability current (T_{MPC}) are calculated in the system of Coulomb potential for $F = 0.5, 0.6, 0.7$ a.u. The blue and grey regions represent the tunneling ionization (TI) and the over-the-barrier ionization (OBI) regimes, respectively, for the case of Coulomb potential. The inset shows the ionization probabilities at crossover times for Coulomb potential (blue line) and square well potential (blue dashed line).

These phenomena are consistent with the behavior of the Bohmian tunneling time [23], and they explain again that the tunneling dynamics has a strong dependence on the actual shape of the barrier. However, the method introducing the crossover time in this work is utterly different from that of the Bohmian tunneling time [23]. Note that we do not refer to the barrier width, which is given approximately by I_{p}/F within the strong field approximation [33–35] and causes the other four tunneling times for hydrogen to become divergent in a relatively intense field [23]. Besides, as compared to the L^{N}, the crossover time calculated by L^{UN} is a bit delayed. But the delayed time reduces as the field strength increases, since the ionization rates in both cases (L^{N} and L^{UN}) at the crossover time are approaching slowly with increasing F. We also display the Keldysh tunnel time τ_k (grey dash-dotted line). For the Coulomb potential, T_{MIV} approaches the Keldysh time at relatively intense field strength. And the full-quantum time T_{MIV} can be comparable with the time T_{MPC}.

In addition, the field strength $F = 0.72(1.13)$ a.u. is the boundary between the TI and the over-the-barrier ionization (OBI) regimes for the system of Coulomb potential (square well potential). However, whether the TI or the OBI, the probability distributions of the bound electron display common behaviors in the temporal evolution [see figures 2(c) and (d) and 3(c) and (d)]. Hence, the crossover time we proposed in this work is applicable in the IT and the OBI regimes, and it seems to make little sense to distinguish between the TI and the OBI when the tunneling dynamics of electrons is discussed fully quantum mechanically. We hope that not only in the TI regime, the attoclock experiment can also be extended to the OBI regime in the future.

5. Conclusion

To summarize, a detailed and systematic study about the overall behavior of the tunneling dynamics of the wave packet in the electronic ground state has been presented. TI occurs at the instant switching on the laser field. For times shorter than the crossover time T_{c}, the ionized wavefunction still couples with the binding potential and its temporal evolution is dominated by the combined effect of binding potential and external field. After the crossover time, the coherence between ionized wavefunction and binding potential fades away, resulting in the escaping parts of wavefunction is solely exposed to the external field and evolves regularly. From the perspective of coupling and decoupling, the crossover time can be explained as the time required for completed ionization of the entire wave packet. For relatively weak fields, this crossover time can be comparable with the cycle duration of central wavelength $\lambda = 800$ nm. Whereas for a time-varying field, based on the well-accepted viewpoint, main contribution of ionization comes from the instant of maximal electric field strength, which means that only parts of electrons are ionized in one-cycle pulse. This indicates that the tunneling time in attoclock experiments reflects the time it takes minor parts of electrons to be ionized.

After the crossover time, the ionized wavefunction decouples with the binding potential, which is a general result and is independent of the form of trapped potentials. Also, the numerical findings rely

exclusively on the analysis of evolution behavior of wave packet, so the method proposed can be directly generalized to the system of quantum dot potential [18, 19]. Thus, our results are universal to some extent for low-dimensional quantum systems. Regardless of the dimensionality, the ionized wavefunction will eventually behaves the same as a free particle in a static field. Then, a regular evolution of wavefunction is expected to appear, perhaps allowing us to generalize the extraction of crossover time from Loschmidt echo function to two- or three-dimensional atomic systems.

Moreover, the constant field is a consequence of adiabatic limit of time-dependent field. For a periodic field, plenty of Floquet states ascribed to the virtual absorption of photons will be involved in the process of TI [36]. Also, the ionized electrons move in the field back and forth, and are even captured by the parent ion. These cause that the ionized wavefunction will possess much richer structures. Whereas, it is possible for the ionized wavefunction to exhibit a periodic structure in the presence of this periodically varying field, which renders us to define a crossover time. This uncertainty issue provides us a motivation to carry on a detailed study in the future.

Acknowledgments

This work is supported by the National Natural Science Foundation of China (Grant Nos. 11725417, 11674393, 12047548, U1930403, U1930201), Science Challenge Project (Grant No. TZ2018005), National Key R & D Program of China (Grant No. 2018YFA0306502).

Data availability statement

All data that support the findings of this study are included within the article.

ORCID iDs

Long Xu https://orcid.org/0000-0001-5314-2799

References

[1] Guéret P, Baratoff A and Marclay E 1987 *Europhys. Lett.* **3** 367–72
[2] Guéret P, Marclay E and Meier H 1988 *Appl. Phys. Lett.* **53** 1617–9
[3] Esteve D, Martinis J M, Urbina C, Turlot E, Devoret M H, Grabert H and Linkwitz S 1989 *Phys. Scr.* **T29** 121–4
[4] Bloch I, Dalibard J and Zwerger W 2008 *Rev. Mod. Phys.* **80** 885–964
[5] Ramos R, Spierings D, Racicot I and Steinberg A M 2020 *Nature* **583** 529–32
[6] Steinberg A M, Kwiat P G and Chiao R Y 1993 *Phys. Rev. Lett.* **71** 708–11
[7] Enders A and Nimtz G 1993 *Phys. Rev.* E **48** 632–4
[8] Mugnai D, Ranfagni A and Ruggeri R 2000 *Phys. Rev. Lett.* **84** 4830–3
[9] Meckel M *et al* 2008 *Science* **320** 1478–82
[10] Tong X M, Zhao Z X and Lin C D 2003 *Phys. Rev. Lett.* **91** 233203
[11] Baker S, Robinson J S, Haworth C A, Teng H, Smith R A, Chirilaă C C, Lein M, Tisch J W G and Marangos J P 2006 *Science* **312** 424–7
[12] Hauge E H and Støvneng J A 1989 *Rev. Mod. Phys.* **61** 917–36
[13] Landauer R and Martin T 1994 *Rev. Mod. Phys.* **66** 217–28
[14] Maji K, Mondal C K and Bhattacharyya S P 2007 *Int. Rev. Phys. Chem.* **26** 647–70
[15] MacColl L A 1932 *Phys. Rev.* **40** 621–6
[16] Eckle P, Pfeiffer A N, Cirelli C, Staudte A, Dörner R, Muller H G, Büttiker M and Keller U 2008 *Science* **322** 1525–9
[17] Eckle P, Smolarski M, Schlup P, Biegert J, Staudte A, Schöffler M, Muller H G, Dörner R and Keller U 2008 *Nat. Phys.* **4** 565–70
[18] McDonald C R, Orlando G, Vampa G and Brabec T 2013 *Phys. Rev. Lett.* **111** 090405
[19] Orlando G, McDonald C R, Protik N H, Vampa G and Brabec T 2014 *J. Phys. B: At. Mol. Opt. Phys.* **47** 204002
[20] Niu Q and Raizen M G 1998 *Phys. Rev. Lett.* **80** 3491–4
[21] Damburg R J and Kolosov V V 1976 *J. Phys. B: At. Mol. Phys.* **9** 3149–57
[22] Zhao R, Sarwono Y P and Zhang R-Q 2017 *J. Chem. Phys.* **147** 064109
[23] Zimmermann T, Mishra S, Doran B R, Gordon D F and Landsman A S 2016 *Phys. Rev. Lett.* **116** 233603
[24] Karkuszewski Z P, Jarzynski C and Zurek W H 2002 *Phys. Rev. Lett.* **89** 170405
[25] Quan H T, Song Z, Liu X F, Zanardi P and Sun C P 2006 *Phys. Rev. Lett.* **96** 140604
[26] Teeny N, Yakaboylu E, Bauke H and Keitel C H 2016 *Phys. Rev. Lett.* **116** 063003
[27] Satya Sainadh U, Sang R T and Litvinyuk I V 2020 *J. Phys. Photonics* **2** 042002
[28] Yakaboylu E, Klaiber M, Bauke H, Hatsagortsyan K Z and Keitel C H 2013 *Phys. Rev.* A **88** 063421
[29] Javanainen J, Eberly J H and Su Q 1988 *Phys. Rev.* A **38** 3430–46
[30] Su Q and Eberly J H 1991 *Phys. Rev.* A **44** 5997–6008
[31] Feit M D, Fleck J A and Steiger A 1982 *J. Comput. Phys.* **47** 412–33
[32] Landau L D and Lifshitz E M 1991 *Quantum Mechanics: Non-Relativistic Theory* (Oxford: Pergamon)

[33] Keldysh L V 1965 *Sov. Phys - JETP* **20** 1307–14
[34] Faisal F H M 1973 *J. Phys. B: At. Mol. Phys.* **6** L89
[35] Reiss H R 1980 *Phys. Rev.* A **22** 1786–813
[36] Shirley J H 1965 *Phys. Rev.* **138** B979